Effects of Urbanization on the water cycle in the Shiyang River Basin: Based on stable isotope method

Rui Li[a,b], Guofeng Zhu[a,b,*], Siyu Lu[a,b], Liyuan Sang[a,b], Gaojia Meng[a,b], Longhu Chen[a,b], Yinying Jiao[a,b], Qinqin Wang[a,b]

Affiliations:

[a] *College of Geography and Environmental Science, Northwest Normal University, Lanzhou 730070, Gansu, China*

[b] *Shiyang River Ecological Environment Observation Station, Northwest Normal University, Lanzhou 730070, Gansu, China*

** Corresponding author. Email: zhugf@nwnu.edu.cn.*

Abstract: In water-scarce arid areas, the water cycle is affected by urban development and natural surface changes,and urbanization has a profound impact on the hydrological system of the basin.Through an ecohydrological observation system established in the Shiyang River basin in the inland arid zone,we studied the impact of urbanization on the water cycle of the basin using isotope methods.The results showed that urbanization significantly changed the water cycle process in the basin, and accelerated the rainfall-runoff process due to the increase of urban land area,and the mean residence time (MRT)of river water showed a fluctuating downward trend from upstream to downstream,and was shortest in the urban area in the middle reaches,and the MRT was mainly controlled by the landscape characteristics of the basin. In addition,our study showed that river water and groundwater isotope data were progressively enriched from upstream to downstream due to the construction of metropolitan landscape dams,which exacerbated evaporative losses of river water, and

also strengthened the hydraulic connection between groundwater and river water around the city.Our findings have important implications for local water resource management and urban planning and provide important insights into the hydrologic dynamics of urban areas.

Keywords: Urbanization; Water cycle; Stable isotopes; River Connectivity

1 Introduction

According to the "2020 Global Cities Report," urban areas are currently home to more than half of the worldwide people, which amounts to 56.2%. This pattern is expected to continue over the course of the next decade, culminating in an urbanization rate of 60.4% by the year 2030. In addition, the study forecasts that by the year 2050, approximately seventy percent of the world's population would reside in urban areas (Chen et al., 2020; UN, 2019; UN-Habitat, 2020). Unlike other regions, urban regions have a substantial influence on the hydrological system, resulting in significant consequences on water balance and the water cycle (Gillefalk et al., 2021). To meet the diverse household and industrial requirements in metropolitan areas, where the population is concentrated and water demands are high, a complex interplay between natural and manmade components of the water cycle is required. These components include both natural features such as streams and groundwater, as well as human-made systems like drinking water and drainage networks (Gessner et al., 2014). Urbanization exacerbates water depletion and has far-reaching impacts on groundwater (Flörke et al., 2018; McDonough et al., 2020), affecting the environment and water availability (Bhaskar and Welty, 2015). Rapid urbanization will seriously

pressure the structure, function and water quality degradation of basin ecosystems (Grimm et al., 2008; Sun and Lockaby, 2012; Sun et al., 2015).

Urbanization's effects on basin hydrology and the related processes have complex and varying consequences (Caldwell et al., 2012; Martin et al., 2017). In the past few decades, with the continuous acceleration of urbanization, human activities in urban areas have become more frequent, and the hydrological effects of urbanization have become more intense, attracting widespread attention worldwide (Salvadore et al., 2015). The rise of impervious surfaces in urbanized regions increases the rate of urban water runoff, which raises the danger of urban floods (Wing et al., 2018). In addition, high-intensity human activities have led to increased discharge of domestic sewage and industrial wastewater, deteriorating water quality and ecological environment (Pickett et al., 2011). Meanwhile, basin water cycle processes are influenced by a combination of meteorological and subsurface factors. It has been found that urbanization has led to significant increases in runoff and peak flows in rivers (Liu et al., 2018; Han et al., 2022) and has resulted in shorter runoff response times (Anderson et al., 2022), which also exacerbates the intensity and frequency of flooding in basins (De Niel and Willems, 2019; Blum et al., 2020). On the other hand, the urbanization process leads to an increase in the amount of rainfall in the basin as well as an increase in the frequency of extreme rainfall events (Shastri et al., 2015; Fu et al., 2019; Yang et al., 2021), whereas in dryland inland river basins in arid zones that are dependent on water resources for development, the impacts of urbanization on the water cycle processes of the basins are still not clear, and they

need to be explored in depth the effects of urbanization on basin water cycle processes. Hence, study into how human activities alter the features of river runoff and the water cycle within a basin is essential for the prudent use and sustainable development of water resources.

Isotopes that are stable of hydrogen and oxygen are very useful tools for investigating hydrological issues that are connected to surface water and groundwater sources (Fekete et al., 2006; Förstel and Hützen, 1983; Vystavna et al., 2021). Researchers have been conducting studies using stable isotopes as tracers over the course of the past few years in order to explore the impact that urbanization has had on the water cycle. Urbanization has the potential to trigger and intensify convective activity and warm-season rainfall in both urban areas and their surrounding regions (Burian and Shepherd, 2005). Researchers generally agree that urbanization reduces depressions on the underlying surface, weakens water permeability and increases runoff. At the same time, the lower roughness of the underlying surface shortens the confluence time (Guan et al., 2015; Oudin et al., 2018). Moreover, against the backdrop of swift urbanization, the swift proliferation of urban regions has resulted in a sharp surge in impermeable areas, alterations to regional microclimates, and the erection of a vast number of infrastructures (including overpasses, subways, and so on), all of which have significantly impacted the water cycle process in urban areas (Jacobson, 2011; Westra et al., 2014). The complex connection between the permeable and impermeable zones influences the surface confluence processes (Bruwier et al., 2020). The construction of urban water conservation projects, such as rubber dams

and pumping stations, also affects the confluence process of urban areas to a certain extent (Zhu et al., 2021). Limited long-term and continuous monitoring has hampered accurate depiction of urbanization's spatiotemporal effects on basin hydrology. Furthermore, the scientific research till lacks sufficient research on arid regions that heavily depend on mountain river runoff for sustenance and development.

Against the background of increasing urbanization, it is particularly important to study the hydrological impacts of urbanization on basins and their corresponding countermeasures, especially in arid inland river basins, where the impacts of human activities in urban areas on rivers may be more prominent. Therefore, the Shiyang River Basin (SYR), located in the inland arid zone of Northwest China, was used as an example to study the impact of urbanization on the hydrology of the basin using the stable isotope method. The following problems are proposed to be solved: (1) An examination of the mechanisms underlying evaporation and infiltration of surface water within urban aquatic ecosystems; (2) Assessing the effects of urbanization on water body connectivity through a comprehensive analysis; (3) The influence of urbanization on the precipitation-runoff process is analyzed. This provides us with essential information on how to maintain and manage the water resources found in inland river basins, which is especially useful in light of the fact that the rate of urbanization is growing.

2 Observation Systems and Data

2.1 Study Area

The SYR Basin is located in Gansu Province, China, to the east of the He-xi Corridor. Its coordinates are 101°22' ~ 104°16' E and 36°29' ~ 39°27' N. The SYR Basin is bounded to the west by the Wushaoling Mountain and to the north by the foothills of the Qilian Mountain (Zhu et al., 2019). The basin in question is situated within the continental temperate belt, characterized by a parched climate and diverse topography. Annual precipitation hovers within the range of 100 to 600 mm, while pan evaporation levels exhibit greater variability, ranging from 700 to 2600 mm annually. The majesty of the Qilian Mountains is where the SYR begins its journey, and the Qilian Mountains are the source of its eight main tributaries. The SYR is principally supported by the convergence of precipitation, snowmelt, and glacier runoff (Wei et al., 2013).

The Wuwei City is crossed by four important rivers, namely the Xiying, Zamu, Huangyang and Jinta, which cover a catchment area of 3986 km^2. As the principal water source for the entire region, the SYR Basin is one of the most highly utilized inland river basins in terms of water resource development and consumption worldwide. The dams in the SYR basin are predominantly situated in close proximity to the urbanized regions of Liangzhou District, located within Wuwei City. Liangzhou District, situated in the middle of the basin, boasts of a relatively high population density and a notable commercial concentration. At the turn of the millennium, Wuwei City only boasted a paltry five landscape dams positioned on its rivers. As of 2019, this figure has surged dramatically, with a staggering total of 51 urban landscape dams now gracing both urban and peri-urban areas of the city. These dams

are primarily composed of man-made landscape waterfalls and rubber dams, fulfilling their core function of creating public landscape water bodies within the urban expanse. (Zhu et al ., 2021).

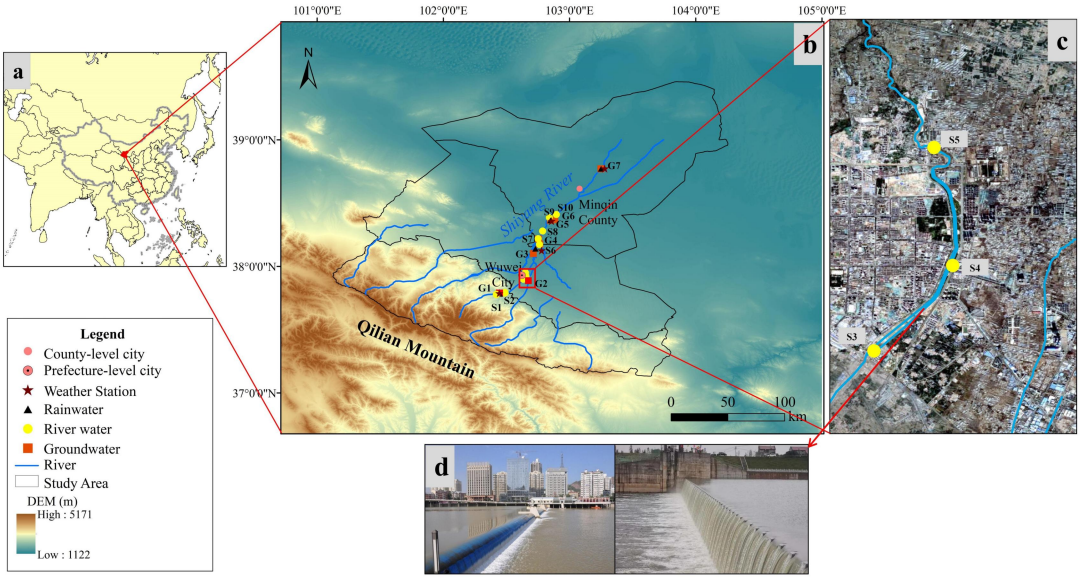

Figure 1 (a) The location of the study area, (b) Comprehensive observation system for the study area, (c) Urban surface water sampling points (from Google Maps), (d) Common urban landscape dams in SYR Basin.

2.2 Sampling and data analysis

Since 2017, a comprehensive observation system has been established in the SYR Basin, and stable isotope observations and hydrometeorological observations have been carried out on surface water, shallow groundwater and rainfall. Continuous sampling in the SYR Basin was carried out from April 2017 to March 2021, different water bodies were sampled, and we collected a total of 943 samples from 24 sampling points (Table 1). The river sampling location ought to be selected such that it is physically possible to go as close to the middle of the river as possible, with the goal of minimizing the impact of areas with standing water and sewage. Artesian well

water was collected as groundwater samples at 7 sampling locations around the basin. The automated weather station was used to measure meteorological factors such as temperature and relative humidity while collecting precipitation samples. Water samples were sealed in high-density polyethylene bottles to avoid evaporation and leakage during transit and storage, precipitation samples were collected using weather station standard rain gauges. These samples were then frozen and wrapped with plastic tape.

Table 1 Basic information on precipitation, surface water and groundwater sampling sites

Parameter	**Sampling Point**	**Number**	**Sampling period**	**Collection Channels**
Precipitation	P1, P2, P3, P4, P5,P6, P7,	387	Precipitation events	Rain tube collection
Surface Water	S1,S2,S3,S4,S5,S6, S7, S8, S9, S10	270	Monthly	Sampling in river water
Groundwater	G1、G2、G3、G4、G5、G6、G7	189	Monthly	Sampling from wells

Analysis of the water samples is conducted through liquid water isotope analysis utilizing the DLT-100 (Los Gatos Research) in the Stable Isotope Laboratory at Northwest Normal University. Each water sample and isotope standard are injected six times in succession to assure reliable findings, with the first two injection values eliminated and the average of the last four injections used for final analysis, thereby avoiding any potential isotope analysis memory effect. The isotope measurements were denoted by the symbol "δ," which indicates the deviation in thousandths from the Vienna Standard Mean Ocean Water:

$$\delta_{\text{sample}}(‰) = [(\frac{R_s}{R_{v-smow}}) - 1] \times 1000 \quad (1)$$

where R_s is the ratio of $^{18}O/^{16}O$ or $^{2}H/^{1}H$ in the collected sample, *Rv-smow* is the ratio of $^{18}O/^{16}O$ or $^{2}H/^{1}H$ of the Vienna standard sample, and the analytical accuracy of δD and δ^{18}O is ±0.6‰ and ±0.2‰, respectively.

3 Methods

3.1 Calculation and indication of *d-excess*

Dansgaard (1964) introduced the concept of deuterium excess (*d-excess*) as the difference in isotopic composition between global precipitation and the Vienna Standard Mean Ocean Water (V_{SMOW}) reference water, which corresponds to a value of 10‰. This parameter reflects the average isotopic composition of air masses associated with precipitation and is widely used to identify atmospheric source regions (Deng et al., 2016). *d-excess* was proposed by Dansgaard (Dansgaard, 1964) and is defined as:

$$d\text{-}excess = \delta D - 8\delta^{18}O \quad (2)$$

3.2 Calculation of evaporation losses of surface water

The losses of surface water through evaporation and the resulting fluctuations in water levels of rivers, lakes, and wetlands are key aspects of the terrestrial water cycle that merit significant attention (Gammons et al., 2006; Hamilton et al., 2005). Evaporation is the primary mechanism of water losses in the water cycle. For river water in dry regions and urban river water that flows slowly due to manmade constraints, evaporation cannot be ignored. Thus, it is vital to address the alteration of urban landscape dam water caused by non-equilibrium isotope fractionation during

evaporation. The provided formula (3) can be used to estimate the rate of evaporative water losses from the body of water in question (Skrzypek et al., 2015):

$$f = 1 - \left[\frac{(\delta - \delta^*)}{(\delta_0 - \delta^*)} \right]^{\frac{1}{m}} \quad (3)$$

The variables in the equation are as follows: f represents the ratio of water lost to evaporation, δ denotes the measured values of the water body located in the urban dam area of Wuwei City, situated in the middle reaches of the SYR and δ_0 represents the initial value of the hydrogen and oxygen stable isotope of the water body. It is widely assumed that the point of intersection between the local meteoric water line (LMWL) and the local evaporation line (LEL) represents the average isotopic composition of the input water body within the basin (Gibson et al., 2005). In the current investigation, the intersection point marked by $\delta^{18}O$ = -7.24‰ and δD = -46.9‰ has been designated as the δ_0 value, while δ^* denotes the maximum isotope enrichment factor and m corresponds to the enrichment slope. The calculation of the above parameters in this paper is realized in Hydrocalculator software (Skrzypek et al., 2015) (http://hydrocalculator.gskrzypek.com). According to studies (Qian et al., 2007), it is more accurate to use $\delta^{18}O$ when calculating the evaporation losses ratio, so this study calculates the f value of SYR water using $\delta^{18}O$ value.

3.3 Periodic regression analysis and the mean residence time (MRT)

Seasonal fluctuations in $\delta^{18}O$ values were analyzed using periodic regression analysis to determine how these values changed over time. This method entailed fitting seasonal sine wave curves to annual $\delta^{18}O$ variations using least squares

optimization (Rodgers et al.,2005):

$$\delta^{18}O = \delta^{18}O_{ave} + A \cdot \left[\cos(c \cdot t - \theta)\right] \quad (4)$$

The modelled $\delta^{18}O$ values and the mean weighted annual measured $\delta^{18}O_{ave}$ values were both utilized in the analysis of seasonal fluctuations in δ^{18}O levels. Additionally, the measured δ^{18}O annual amplitude (A), the radial frequency of annual fluctuations (c), and the time in days after the start of the sampling period (t) were also considered in this analysis. Furthermore, the phase lag or time of the annual peak δ^{18}O in radians (θ) was determined through this approach.

An exponential model was used for the purpose of estimating the mean residence time (MRT). This model operates on the presumption that precipitation inputs quickly mix with resident water. In order to do this, the following equation was used (Maloszewski et al., 1983; Rodgers et al., 2005):

$$MRT = c^{-1} \cdot \left[(A_{Z2} / A_{Z1})^{-2} - 1\right]^{0.5} \quad (5)$$

The amplitude of precipitation (A_{Z1}), the amplitude of the surface water outputs (A_{Z2}), and the radial frequency of the annual fluctuation (c) as defined in Eq. (4) were taken into consideration to estimate the mean residence time (MRT).

4 Results

4.1 Spatiotemporal distribution of isotopes in different water bodies

The isotopes values of the surface water in the SYR Basin show a clear enrichment from upstream to downstream when viewed from space. It is worth noting that landscape dams and reservoirs in urban areas alter this pattern significantly, producing markedly higher isotopic compositions of surface water around such structures (Fig. 2). To be more specific, the surface water throughout the entire basin

had average isotope values that were lower than those of the sampling points in the dams region, which had values that were greater (Table 2). In addition, the dams slowed the flow of the river, this resulted in isotope enrichment of the river water. Notably, these values exhibit spatial and temporal variability, with the largest δD and δ^{18}O values observed in river water, and the lowest in groundwater.

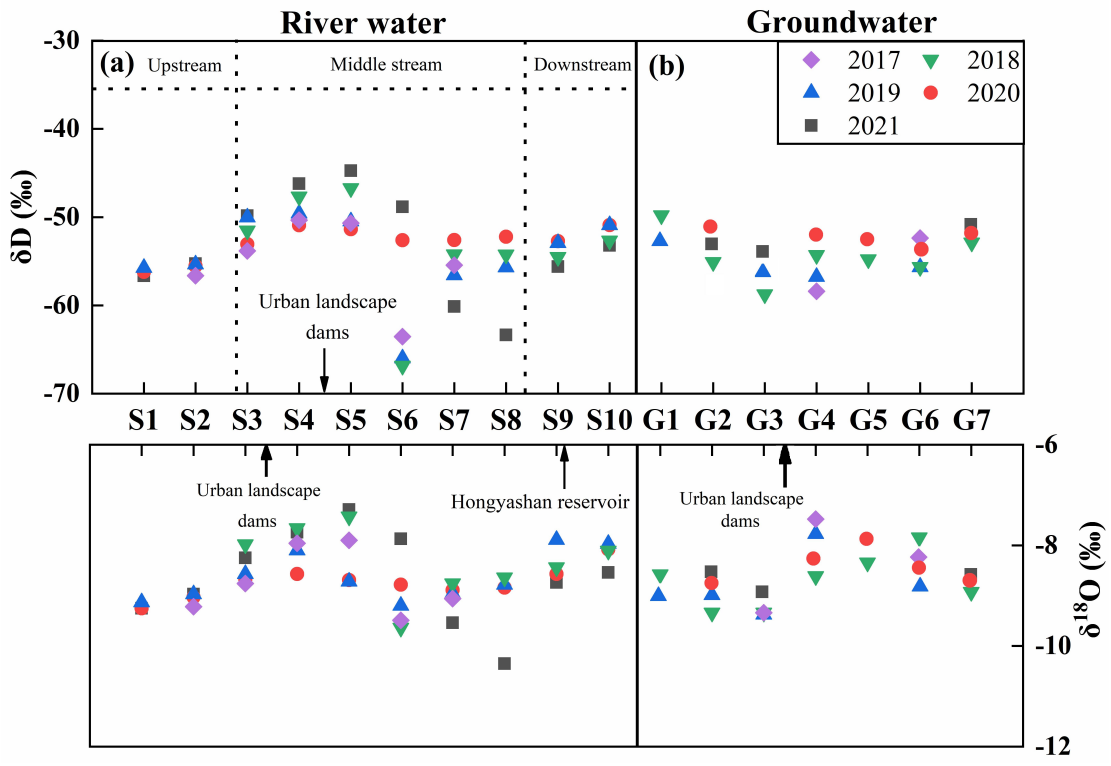

Figure 2 Longitudinal variation of δD and δ^{18}O in river water and groundwater in the SYR Basin.

To be more specific, over the course of time, these values shift seasonally from spring to autumn (Table 2, Fig. 3). There was a range of values from -75.43‰ to -40.62‰ for the δD values of surface water, with an average of -53.53‰. The δ^{18}O values display a varied range, from -10.43‰ to -5.53‰, with an average of -8.54‰, whereas the *d-excess* values demonstrate variability ranging from 10.26‰ to 29.72‰, with 15.28‰ as the average value. A broad spectrum of δD values are observed during the summer season, ranging from -61.27‰ to -31.16‰, with an average

-48.90‰. Meanwhile, $\delta^{18}O$ values fluctuate between -9.52‰ and -3.41‰, with an average -8.12‰. The phenomenon that was observed can be traced back primarily to the aftereffects of the Hongyashan Reservoir built downstream. Because the reservoir has such a large capacity for water retention, it causes significant amounts of river water to evaporate in summer, which ultimately results in a discernible enrichment of the isotopic composition. In both surface water and groundwater, δD and $\delta^{18}O$ showed significant seasonal variations (Fig. 3). Seasonal variations were more pronounced in surface water than in groundwater, with surface water showing the largest amplitude in spring and the smallest amplitude in fall, while groundwater showed closer amplitudes in all seasons, which also indicates that groundwater is less disturbed.

Table 2 Isotopic composition statistics of surface water in SYR Basin

Sampling Point	$\delta^{18}O$			δD			*d-excess*		
	Mean	Min.	Max.	Mean	Min.	Max.	Mean	Min.	Max.
S1	-9.35	-9.86	-9.06	-57.16	-59.46	-52.47	17.2	12.33	23.91
S2	-9.22	-10.02	-8.78	-56.62	-63.85	-10.02	16.46	15.53	19.28
S3	-7.74	-9.03	-7.75	-49.84	-50.76	-46.66	15.42	13.59	19.48
S4	-7.29	-8.79	-7.65	-46.22	-53.29	-46.26	14.9	11.01	18.03
S5	-7.43	-9.11	-5.53	-48.84	-56.66	-40.62	14.29	14.21	29.72
S6	-9.54	-10.43	-8.29	-60.14	-75.43	-54.40	14.31	10.26	17.62
S7	-9.04	-9.54	-8.21	-54.23	-70.04	-48.03	16.54	12.81	21.16
S8	-9.15	-10.35	-8.64	-56.37	-63.35	-52.22	16.84	14.56	19.54
S9	-8.41	-9.70	-6.02	-53.95	-65.33	-45.54	13.33	12.31	19.50
S10	-8.18	-8.84	-6.58	-51.92	-58.05	-45.39	13.48	12.21	21.72

4.2 The Relationship between δD and $\delta^{18}O$ values

As shown by the linear fitting equation $\delta D = 7.52\delta^{18}O+7.58$, there is a significant linear positive correlation ($R^2 = 0.96$) between δD and $\delta^{18}O$ in atmospheric precipitation in the SYR Basin (Fig. 3). It is clear that the slope (7.52) and intercept (7.58) of the local meteoric water line (LMWL) are smaller than the global meteoric

water line (GMWL), which can be attributed to the basin's location in an inland arid region, where precipitation disturbances are less frequent and evaporative fractionation of precipitation is stronger. On the other hand, compared with the slopes of the LMWL, the slopes of the surface water line (SWL) and the groundwater line (GWL) are relatively close (Fig. 3), indicating that there is a strong hydraulic connection between groundwater and river water in the SYR basin, and the slopes of GWL and RWL show GWL > RWL in all seasons, suggesting that the river water is most affected by evaporation and groundwater is less affected by evaporation. In addition, both surface water and groundwater sampling points were distributed near the LMWL, indicating that both river water and groundwater receive recharge from precipitation. Overall, the H-O isotopic composition of surface water samples from the SYR showed a linear regression of $\delta D = 5.63\delta^{18}O - 6.11$, and the slope of RWL was the largest in the autumn (slope = 6.65) and the smallest in the summer (slope = 5.56), which indicated that the river water evaporated the weakest in the autumn and the strongest in the summer.

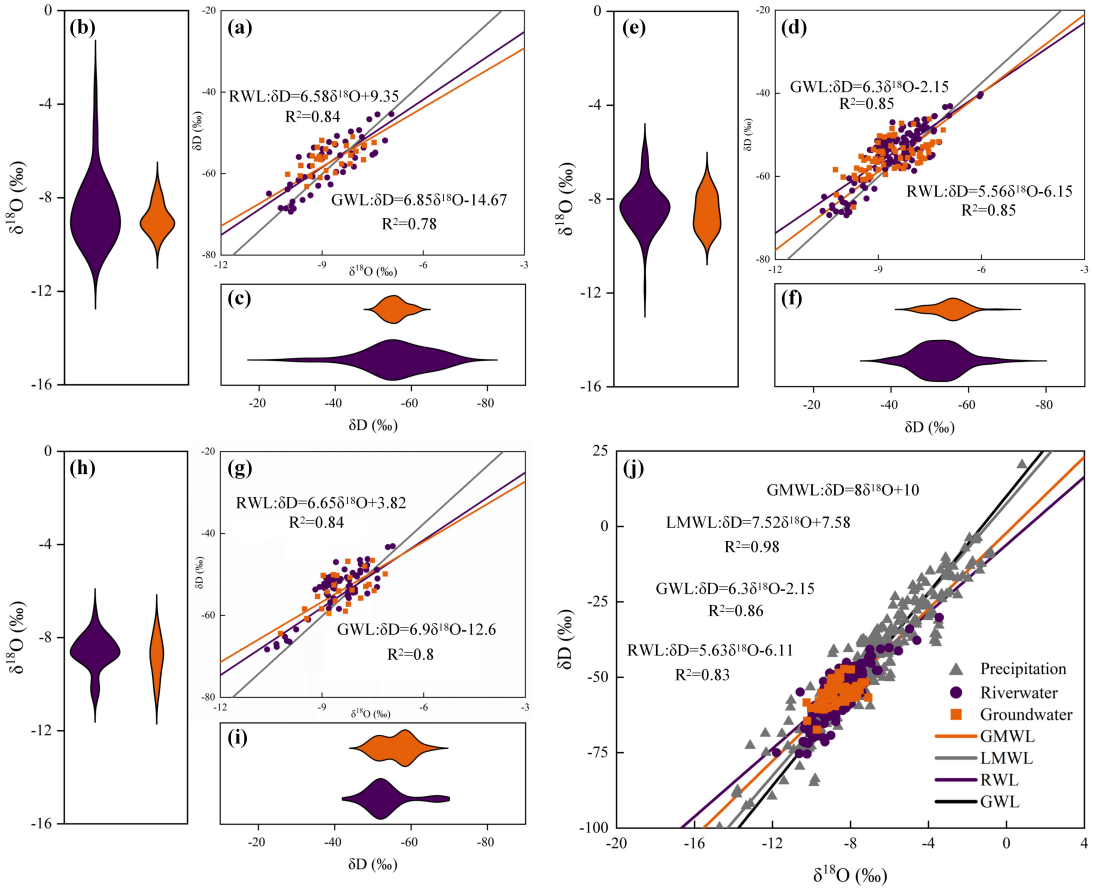

Figure 3 Relationship between δD and δ18O in various water bodies in the SYR Basin during different seasons (a,d,g represent spring, summer, autumn; j represent the comparison of RWL, GWL, LMWL and GMWL during the entire sampling period;.b-c, e-f, h-i represent the distribution of δD and δ^{18}O in river water and groundwater in spring, summer and autumn).

Isotopic analysis of groundwater samples reveals a range of δD and δ18O values spanning from -50.7‰ to -71.9‰ and from -7.23‰ to -10.4‰, respectively. Moreover, the groundwater samples analyzed in the study displayed a linear regression of $\delta D=6.3\delta^{18}O-2.15$ ($R^2=0.86$). And it is interesting to note that groundwater also shows significant enrichment near the urban landscape dams (Fig. 2), indicating that groundwater is also affected by evapotranspiration, mainly because the Wuwei urban area is in the region of a large alluvial fan in front of the mountains, the sand and gravel aquifers are very permeable, and the depth of groundwater burial

290 is shallow, making the groundwater more susceptible to the effects of evaporation.

291 **4.3 Impact of urbanization on groundwater**

292 We compared monthly variations in isotopic values of groundwater near the city
293 with monthly variations in river water from a landscaped dam and found that the
294 monthly variations in groundwater near the city were closely related to river water
295 from a landscaped dam. The concentration of groundwater sampling sites near the city
296 near the sampling sites of the dam water indicates that the groundwater around the
297 city has similar isotopic signatures to the dam and river water (Fig. 4). This suggests
298 that groundwater near the city is recharged by river water during the summer months.
299 In addition, we demonstrated this by comparing the data of the dam river water with
300 the groundwater level. In addition, a portion of the groundwater sampling sites around
301 the city are located in the lower right corner of the LMWL, which suggests that the
302 groundwater around the city may also experience some degree of evaporation.

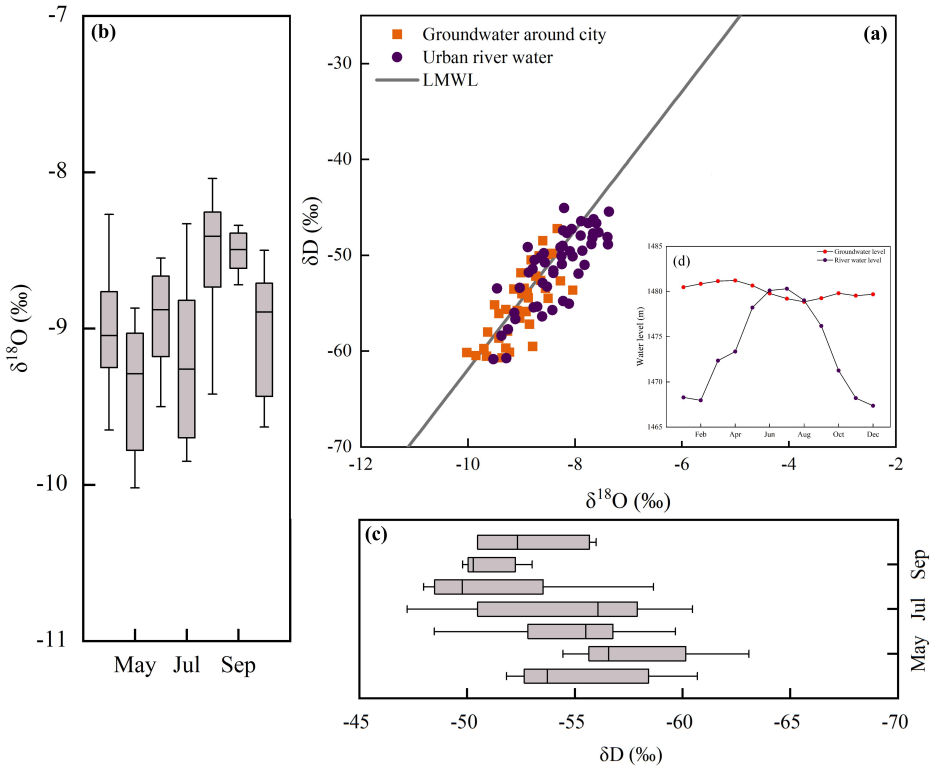

Figure 4 (a) Relationship between $\delta^{18}O$ and δD of groundwater around city and urban river water; (b) Monthly variations of $\delta^{18}O$ in groundwater around city; (c) Monthly variations of δD in groundwater around city.

In addition, we also compared and analyzed the changes of groundwater isotope values with those of groundwater around the city in the whole basin, and found that there was a close correlation between the changes of groundwater around the city and those of the river, while the other groundwater isotope values did not have a strong correlation with the river (Fig. 5). In the urban area, the mean values of δD and $\delta^{18}O$ of the dammed river water were -8.26‰ and -49.88‰, respectively, while the mean values of δD and $\delta^{18}O$ of the groundwater around the city were -8.44‰ and -50.36‰, respectively, which indicated that the δD and $\delta^{18}O$ values of the groundwater around the city were similar to those of the river water in the dammed city. In addition, the isotopic mean values of δD and $\delta^{18}O$ of groundwater throughout the SYR basin were

317 -8.73‰ and -54.78‰, which are significantly different from the isotopic values of
318 river water in the urban dam.

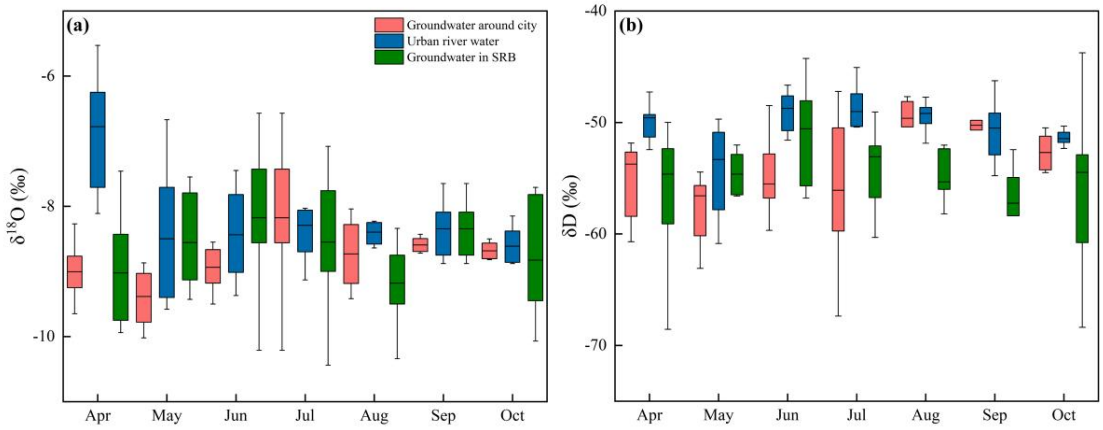

319

320 Figure 5 (a) Monthly variations of $\delta^{18}O$ in urban river water and groundwater around city, (b)
321 Monthly variations of δD in urban river water and groundwater around city.

322 **4.4 Temporal and spatial variation of surface water evaporation losses in the**
323 **urban area of Wuwei**

324 In addition to being an essential part of the hydrological cycle, evaporation is
325 widely recognized as one of the most significant factors driving climate change in
326 semi-arid regions and in telluric ecosystems (Gibson et al., 2002; Gibson and Edwards,
327 2002). An obviously spatial and temporal fluctuation can be seen in the amount of
328 surface water that is lost to evaporation in the upper mountain area as well as the
329 intermediate urban area of the SYR basin (Fig. 6). Analyzed from a time-varying
330 perspective, there is significant seasonal variation in surface water evaporation losses
331 both in the upstream mountainous region and the midstream urban area of Wuwei,
332 with the highest rates occurring during summer and the lowest during winter (Fig.6).
333 Additionally, a spatial comparison reveals that surface water evaporation losses in the
334 midstream urban area of Wuwei are significantly greater than those in the upstream

mountainous area.

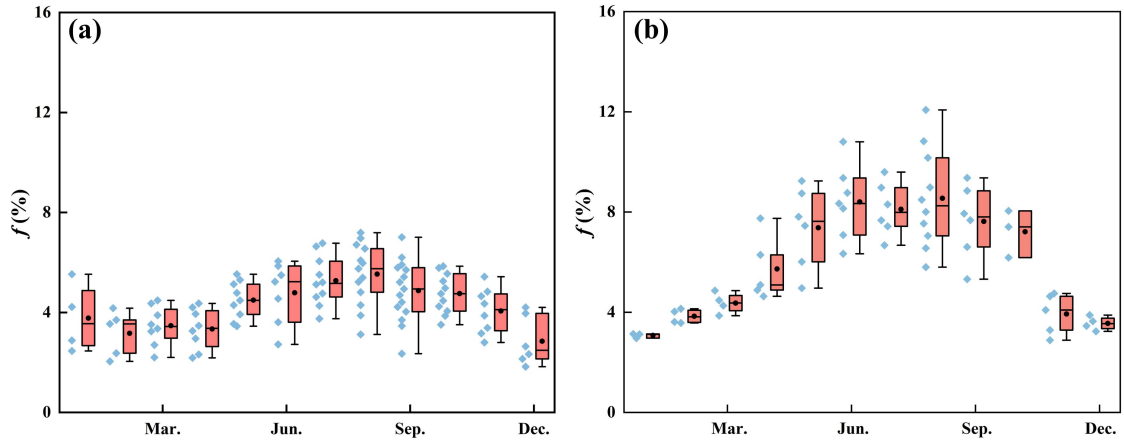

Figure 6 Evaporation losses from surface water in different areas of the SYR (a) Upper reaches mountainous area, (b) Middle reaches urban areas.

Differences contributing to evaporation losses from the river in the upstream and midstream urban areas can be explained mainly by the landscape characteristics of the basin. In the upstream of the Shiyang River, higher vegetation cover and atmospheric humidity in the mountainous areas result in weaker evaporation losses, while the midstream are dominated by urban land, and urban landscapes increase the watershed area and slow down the river, exacerbating evaporation losses from the river.

5 Discussion

5.1 Effects of Urbanization on the Rainfall-Runoff Process

Fig. 7 depicts the regression model of rainfall events in the SYR Basin, represented by a sine wave, and the fitting of surface water $\delta^{18}O$ across the research season. The $\delta^{18}O$ levels of precipitation reported in the SYR Basin have an excellent regularity (R^2=0.46) and a seasonal patterns trend that effectively depicts the nfluence of the monsoon climate on the local environment (Zhu et al., 2019). Seasonal variations are seen in the generally steady $\delta^{18}O$ and $\delta^{18}O$ values of the upstream water.

These results indicate that the predominant component of the river water is the baseflow resulting from recent precipitation runoff. Throughout the duration of the study, the majority of the lowest $\delta^{18}O$ values in the 10 surface water sample points were recorded during the winter, whilst the highest values were recorded during the summer. These trends coincide with both the temporal variation of precipitation isotopes in the SYR Basin, indicating that precipitation input is the underlying cause of isotope changes in river water. Nevertheless, variations in the isotopes of river water differ in range across various regions within the SYR Basin, with significant variation in the degree of fit for the regression curve. The fitting degree of surface water in the upper and lower reaches is relatively low (R^2=0.37, R^2=0.28, R^2=0.23), implying limited seasonal isotopic variability in these regions. The midstream surface water exhibits a notably higher degree of conformity as compared to its upstream and downstream counterparts (R^2=0.38, R^2=0.48, R^2=0.62, R^2=0.78, R^2=0.54, R^2=0.48, R^2=0.52). Moreover, the isotopic composition of surface water throughout this area exhibits notable cyclic variations.

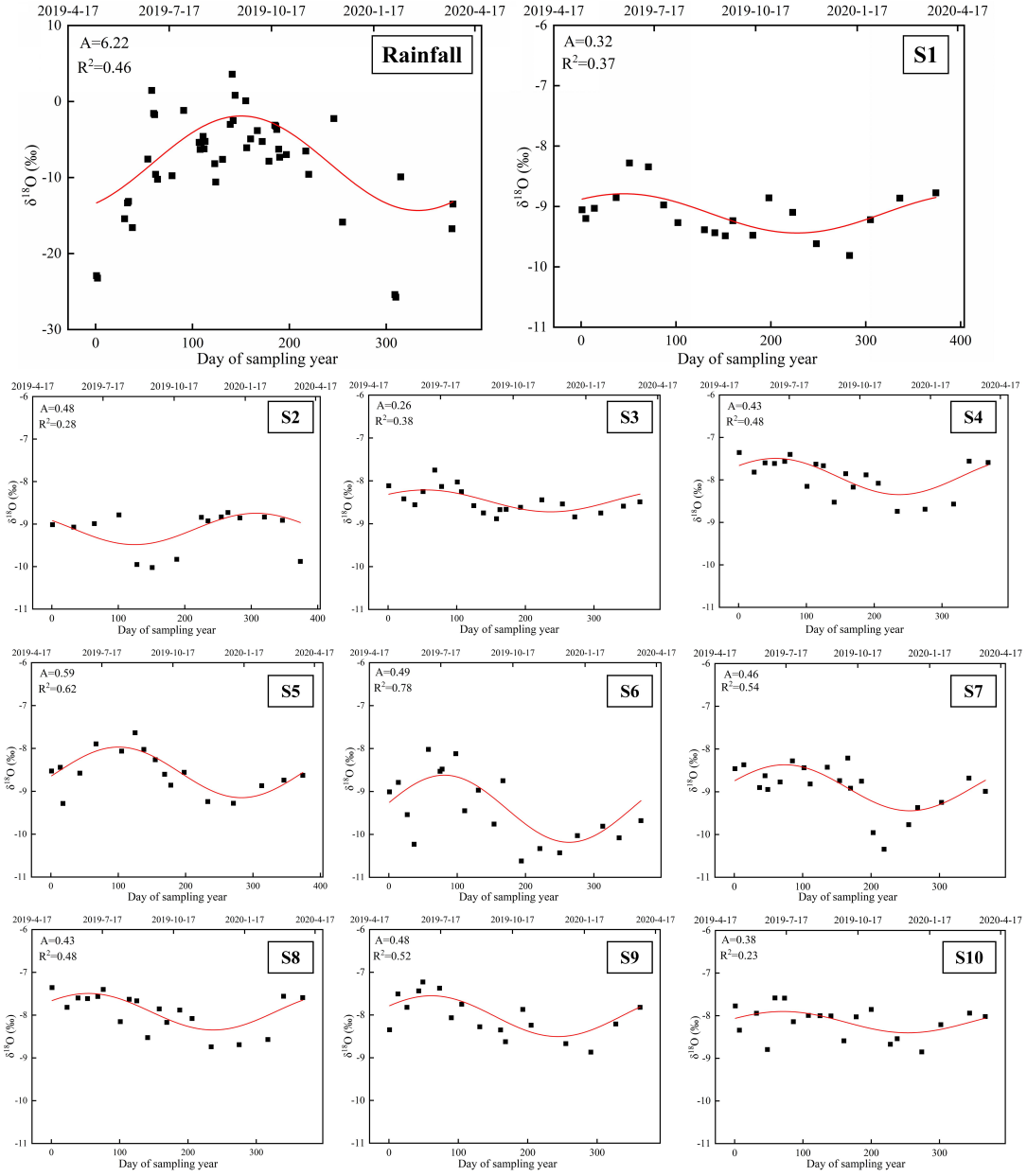

Figure 7 Fits the annual regression model of $\delta^{18}O$ in SYR Basin precipitation and river water (time: 2019/4/17—2020/4/23; S1-S10 are surface water sampling points).

The reasons for differences in isotope periodicity in different regions may be attributed to local water management systems, topographic features and urban development. At points S1, S2, and S10, the correlation of model simulations was low, which could be attributed to the presence of Xiying Reservoir in the upstream as well as Hongyashan Reservoir in the downstream (Sang et al., 2023), where seasonal

variations in the isotope values of the river water are interfered by the reservoir dispatching activities. At points S3 to S5, the correlation of the model simulation is higher, which is because in the middle reaches of the SYR basin, the expansion of urban built-up areas leads to a significant increase in surface runoff during the rainy season, and according to the land use data, the land area of the towns in Wuwei City has continued to increase by 134.38 km^2 from 2010 to 2018, resulting in the surface water showing a cyclical trend comparable to that of the precipitation. Since the 1950s, in order to better utilize water resources, 13 small and medium-sized reservoirs with a total storage capacity of 900,000 m^3 were constructed during this period (Ma et al., 2010), increasing the proportion of rainfall in the runoff constituents as a result of The correlation of the model simulation is at a high level at points S6~S9, where, in contrast to the high-elevation areas in the upper reaches, the terrain in the middle and lower reaches of the SYR basin is relatively flat, mainly with cultivated land and deserts, and is less disturbed by human activities (Sun et al., 2021), which further reflects the responsiveness to recent precipitation inputs.

The Dunnett's test revealed a significant difference ($P < 0.05$) between the MRT of the river and the annual magnitude of $\delta^{18}O$ of the river. We further investigated the relationship between the estimated mean residence time and basin landscape features such as topography (Fig. 8). Using the digital elevation model (DEM) to calculate the mean slope of the SYR basin, we found that the mean residence time was also strongly correlated with the mean basin slope ($R^2 = 0.63$), and that the upper reaches of the Shiyang River basin are mainly high-elevation mountainous areas, where the

topography is sloped, but where the vegetation cover is high and dominated by alpine meadows, subalpine scrub and Qinghai spruce (Zhang et al. 2023), the greater slope leads to a higher gravitational potential, which tends to result in a negative correlation with mean residence time (McGuire et al., 2005), which also contributes to the potentially higher MRT values in the upstream mountains. In our study, catchment area (CA) had a low correlation with MRT (R^2 = 0.40), and a weak relationship between catchment area and MRT has been observed in other studies (McGlynn et al., 2003; McGuire et al., 2005).

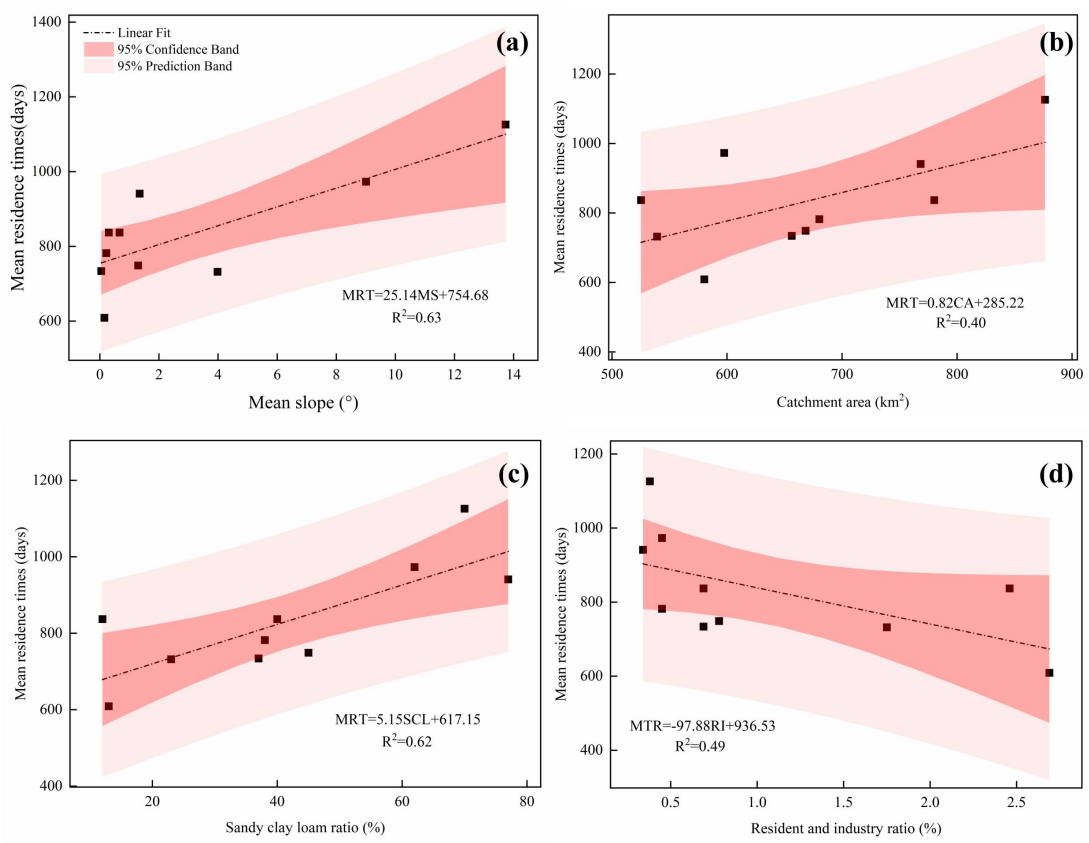

Figure 8 Correlation between MRT and (a) mean slope of the basin, (b) catchment area, (c) sand clay loam ratio, and (d) percentage area of residential and industrial use in the basin, with 95% Confidence and Prediction bands.

Soil is an important component of basin hydrology, and the physical properties

411 of soil, such as water-holding capacity and pore space distribution, have an important
412 influence on the response to precipitation in the basin and the sand-clay-loam soil
413 ratio is used here to investigate the possible relationship with MRT. The results
414 showed that the content of sand clay loam ratio showed a strong positive correlation
415 with MRT (R^2=0.62). Wuwei City is located in the pre-mountain flood-fan belt, and
416 the soil is dominated by sandy soil (Zhang et al., 2023), which is loose in texture, has
417 good permeability and good water retention properties, and is mainly used for
418 agricultural cultivation. Its good permeability increases the vertical movement of
419 water and the length of flow paths, leading to a longer MRT. There is a strong
420 negative correlation between the MRT and the ratios of resident and industrial areas
421 (RI) (R^2=0.49), which also indicates that as urbanization progresses, with the increase
422 of urban land, this undoubtedly leads to a significant shortening of the MRT. However,
423 the MRT in the mid-river urban area is not much shorter as compared to the
424 downstream, which may be attributed to the fact that the mid-river The large number
425 of landscape dams constructed in the urban areas, currently 51 urban landscape dams
426 have been built in the peri-urban areas of Wuwei City, and the considerable number of
427 landscape dams may have counteracted the impact of the urban land use, resulting in a
428 lengthening of the MRT in the middle reaches as well.

429 **5.2 Effects of Water Conservancy Projects in Urban Areas on Isotope Dynamics**

430 Recent studies have suggested that the development of dam-reservoir systems
431 may result in river fragmentation and modifications in flow regimes in terms of their
432 volume,frequency,and duration (Négrel et al., 2016; Murgulet et al., 2016; Peñas and

Barquín, 2019; Maavara et al., 2020). Furthermore, chemical-containing nutrient migration, such as phosphorus, may occur during sediment movement, resulting in widespread eutrophication problems (Yang et al., 2007; Duan et al., 2019). As of 2019, a total of 51 urban landscape dams, primarily consisting of artificial landscape waterfalls and rubber dams, have been constructed in and around Wuwei city (Zhu et al., 2021). In the metropolitan coast of Wuwei, many landscape dams have led to isotopic enrichment in surface water. This damping effect has been observed in numerous dammed rivers across the globe, including the Rio Grande in the southwestern United States (Vitvar et al., 2007) and the Ebro River in Spain (Négrel et al., 2016), as evidenced by isotopic tracers. In the metropolitan coast of Wuwei, a number of landscape dams have led to the enrichment of isotopic tracers in the surface water. The results indicate that the δD and δ^{18}O levels of the surface water at the outflow of Wuwei City are greater than those at the inflow (Fig. 2). Moreover, the influence of evaporation on isotopic composition should not be overlooked, as it can lead to a decrease in *d-excess* values (Peng et al., 2012). Consistent with previous studies (Wang et al., 2019), we observed that the *d-excess* of influent water was higher than that of urban river water (Fig. 9). This observation further supports the accumulation of heavy H-O isotopes in the surface waters of the dam areas, as shown in Fig. 9a. In contrast, due to the confluence of tributaries prior to the S7 sampling point, the river water has lower isotopic values, resulting in elevated *d-excess* values between S6 and S8.

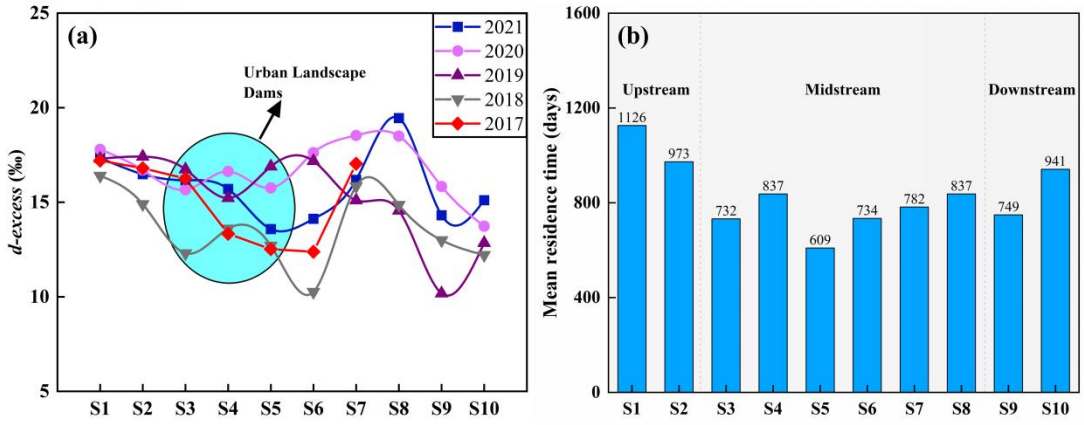

Figure 9 (a) The longitudinal variation of the surface water *d-excess* of the SYR, (b) The longitudinal variation of the surface water MRT of the SYR.

5.3 Effects of Urbanization on the Water Cycle of basins

Localized microclimates in urban areas allow for changes in precipitation and evapotranspiration processes, while urbanization alters the pristine subsurface, complicating water cycle processes in the basin (Jacobson, 2011; Westra et al., 2014; Oudin et al., 2018). In terms of the impact on runoff, it is mainly reflected in the increase of surface impermeability due to urbanization, the land use area of Wuwei urban land increased by about 134.38 km^2 from 2010 to 2018, which greatly weakened the infiltration process in urban areas, and the rainfall runoff process simulated by sinusoidal cyclic regression method showed that there were significant differences in the river metro in different parts of the Shiyang River Basin, and that the middle reaches of the river had the highest degree of urbanization, and the time of the metro was the shortest, which further increases the contribution of rainfall to runoff. Regarding the effect of urbanization on evapotranspiration, a large number of dams were constructed on the Shiyang River and flowed through the urban area of Wuwei, causing significant evapotranspiration losses, in addition, these landscape

dams also led to hydrogen and oxygen isotope enrichment, and the numerous reservoirs that were constructed for the construction and development of the city (Ma et al., 2010), and these reservoirs also contributed to a significant evapotranspiration loss effect, which has been previously confirmed in our study was also confirmed (Sang et al., 2023). On the other hand, our study found that the isotopic compositions and trends of urban nearshore groundwater were similar to those of surface water, which suggests that there is a close correlation between urban nearshore groundwater and river water, and that the difference in water levels between river water and groundwater may be the main reason for river recharge of urban nearshore groundwater (Fig. 4). In the rainy season, the river level gradually rises, which decreases the difference between the water levels of urban nearshore groundwater and river water, and the river water recharges the groundwater, and in the dry season, the river level decreases, and the urban nearshore groundwater, which is buried at a shallow depth, in turn recharges the river.

In addition, the growth of urbanization has had a dramatic impact on the water environment in cities, where water problems occur frequently (Giri and Qiu, 2016; Ma et al., 2022). Urbanization has increased impervious surfaces such as parking lots, rooftops, roads, and sidewalks, leading to increased runoff, which creates additional pathways for pollutants to be transported from landscapes to water bodies (Ren et al., 2014; Wilson and Weng, 2010; Nolan et al., 2023). On the other hand, agricultural activities have increased some of the fertilizers, pesticides, herbicides and dairy manure in the farmland into the nearest water bodies, which can directly and

indirectly affect will reduce water quality (Yu et al., 2013). The Shiyang River Basin in the Northwest Arid Zone is an inland river basin with the highest development intensity and the sharpest conflict between water supply and demand in the region. The Liangzhou district in the central part of the Shiyang River basin is the most densely populated artificial oasis with the largest scale of water demand in the entire basin. Our previous study found that direct discharge of industrial and community domestic wastewater into the river led to deterioration of surface water quality around the Shiyang River basin (Ma et al., 2021). In addition agricultural activities have less impact on the upper reaches of the Shiyang River and relatively more impact on the middle and lower reaches , and the application of nitrogen-based fertilizers during agricultural cultivation is the main cause of high $NH4^{+}$ and $NO3^{-}$ concentrations in the area (Ma et al., 2021), which may also lead to increased salinity and accelerated eutrophication of the river, threatening the safety of the basin's water environment. Overall, human activities (urbanization) may alter the water cycle processes inherent in inland river basins, and the implications of such changes need to be further explored.

6 Conclusions

In this study, we investigated the hydrometeorological and isotopic data of the Shiyang River Basin from 2017 to 2021, and our investigations showed that urbanization had a significant impact on the water cycle of the basin.The results showed that the isotopic values of the river water showed a significant enrichment from upstream to downstream, but facilities such as landscape dams and reservoirs in

the urban area significantly altered this natural pattern, and the isotopic values of the river water in the urban area (δD=-48.31‰; δ^{18}O=-7.49‰) were higher than those of the natural river water (δD=-55.77‰; δ^{18}O=-8.98‰), and landscape dams aggravated the evaporation losses of river water, due to the increase of urban land area, which accelerated the rainfall-runoff conversion process, the residence time of surface water in different regions of the Shiyang River Basin had obvious differences, and the MRT from the upstream to the downstream showed a fluctuating downward process, which was shortened from 1,126 days in the upstream to 941 days in the downstream, and the MRT was mainly controlled by the basin's landscape features. In addition, there was a strong relationship between the isotopic composition of the reservoir and the surrounding groundwater. Overall, urbanization has a profound impact on the hydrological system of the basin, and the results of this study can provide some references for future research on urbanization and the water cycle, and improve our understanding of the hydrological processes of basin in arid zones.

Acknowledgements

This research was financially supported by the National Natural Science Foundation of China (41971036, 41867030).

Author contributions statement

Rui Li: Writing-Original draft preparation; Guofeng Zhu: Writing-Reviewing and Editing; Siyu Lu: Methodology; Liyuan Sang and Gaojia Meng: Data processing and Experiment; Longhu Chen and Yinying Jiao: Methodology and visualization; Qinqin Wang : Visualization;

Data availability Statement

The isotopic data that support the findings of this study are openly available in Zhu, Guofeng (2022), "Stable water isotope monitoring network of different water bodies in SYR Basin, a typical arid river in China", Mendeley Data, V1, doi: 10.17632/vhm44t74sy.1. The source of soil data comes from the Harmonized World Soil Database (HWSD) constructed by the Food and Agriculture Organization of the United Nations (FAO) and the International Institute for Applied Systems (IIASA) on 2009. The land-use and land-cover change data of the Shiyang River Basin were obtained from Chinese Academy of Sciences, the data centre of resources and environmental science (http://www.resdc.cn).

Competing Interests

We undersigned declare that this manuscript entitled "Effects of Urbanization on the water cycle in the SYR Basin: Based on stable isotope method" is original, has not been published before and is not currently being considered for publication elsewhere.

The authors declare that they have no known competing financial interests or personal relationships that could have appeared to influence the work reported in this paper.

Reference

Anderson, B. J., Slater, L. J., Dadson, S. J., Blum, A. G., and Prosdocimi, I.: Statistical Attribution of the Influence of Urban and Tree Cover Change on Streamflow: A Comparison of Large Sample Statistical Approaches, Water Resources Research, 58, e2021WR030742, https://doi.org/10.1029/2021WR030742, 2022.

561 Asano, Y., Uchida, T., and Ohte, N.: Residence times and flow paths of water in steep
562 unchannelled catchments, Tanakami, Japan, Journal of Hydrology, 261, 173–192,
563 https://doi.org/10.1016/S0022-1694(02)00005-7, 2002.
564 Baker, A.: Land Use and Water Quality, in: Encyclopedia of Hydrological Sciences,
565 edited by: Anderson, M. G. and McDonnell, J. J., John Wiley & Sons, Ltd,
566 Chichester, UK, hsa195, https://doi.org/10.1002/0470848944.hsa195, 2005.
567 Bhaskar, A. S. and Welty, C.: Analysis of subsurface storage and streamflow
568 generation in urban basins, Water Resour. Res., 51, 1493–1513,
569 https://doi.org/10.1002/2014WR015607, 2015.
570 Blum, A. G., Ferraro, P. J., Archfield, S. A., and Ryberg, K. R.: Causal Effect of
571 Impervious Cover on Annual Flood Magnitude for the United States,
572 Geophysical Research Letters, 47, e2019GL086480,
573 https://doi.org/10.1029/2019GL086480, 2020.
574 Bruwier, M., Maravat, C., Mustafa, A., Teller, J., Pirotton, M., Erpicum, S.,
575 Archambeau, P., and Dewals, B.: Influence of urban forms on surface flow in
576 urban pluvial flooding, Journal of Hydrology, 582, 124493,
577 https://doi.org/10.1016/j.jhydrol.2019.124493, 2020.
578 Burian, S. J. and Shepherd, J. M.: Effect of urbanization on the diurnal rainfall pattern
579 in Houston, Hydrol. Process., 19, 1089–1103, https://doi.org/10.1002/hyp.5647,
580 2005.
581 Caldwell, P. V., Sun, G., McNulty, S. G., Cohen, E. C., and Moore Myers, J. A.:
582 Impacts of impervious cover, water withdrawals, and climate change on river

583 flows in the conterminous US, Hydrol. Earth Syst. Sci., 16, 2839–2857,
584 https://doi.org/10.5194/hess-16-2839-2012, 2012.
585 Chen, G., Li, X., Liu, X., Chen, Y., Liang, X., Leng, J., Xu, X., Liao, W., Qiu, Y., Wu,
586 Q., and Huang, K.: Global projections of future urban land expansion under
587 shared socioeconomic pathways, Nat Commun, 11, 537,
588 https://doi.org/10.1038/s41467-020-14386-x, 2020.
589 Dansgaard, W.: Stable isotopes in precipitation, Tellus, 16, 436–468,
590 https://doi.org/10.1111/j.2153-3490.1964.tb00181.x, 1964.
591 De Niel, J. and Willems, P.: Climate or land cover variations: what is driving observed
592 changes in river peak flows? A data-based attribution study, Hydrol. Earth Syst.
593 Sci., 23, 871–882, https://doi.org/10.5194/hess-23-871-2019, 2019.
594 Deng, K., Yang, S., Lian, E., Li, C., Yang, C., and Wei, H.: Three Gorges Dam alters
595 the Changjiang (Yangtze) river water cycle in the dry seasons: Evidence from
596 H-O isotopes, Science of The Total Environment, 562, 89–97,
597 https://doi.org/10.1016/j.scitotenv.2016.03.213, 2016.
598 Duan, W., Hanasaki, N., Shiogama, H., Chen, Y., Zou, S., Nover, D., Zhou, B., and
599 Wang, Y.: Evaluation and Future Projection of Chinese Precipitation Extremes
600 Using Large Ensemble High-Resolution Climate Simulations, Journal of Climate,
601 32, 2169–2183, https://doi.org/10.1175/JCLI-D-18-0465.1, 2019.
602 Fekete, B. M., Gibson, J. J., Aggarwal, P., and Vörösmarty, C. J.: Application of
603 isotope tracers in continental scale hydrological modeling, Journal of Hydrology,
604 330, 444–456, https://doi.org/10.1016/j.jhydrol.2006.04.029, 2006.

605 Flörke, M., Schneider, C., and McDonald, R. I.: Water competition between cities and
606 agriculture driven by climate change and urban growth, Nat Sustain, 1, 51–58,
607 https://doi.org/10.1038/s41893-017-0006-8, 2018.
608 Förstel, H. and Hützen, H.: Oxygen isotope ratios in German groundwater, Nature,
609 304, 614–616, https://doi.org/10.1038/304614a0, 1983.
610 Fu, X., Yang, X., and Sun, X.: Spatial and Diurnal Variations of Summer Hourly
611 Rainfall Over Three Super City Clusters in Eastern China and Their Possible
612 Link to the Urbanization, JGR Atmospheres, 124, 5445–5462,
613 https://doi.org/10.1029/2019JD030474, 2019.
614 Gammons, C. H., Poulson, S. R., Pellicori, D. A., Reed, P. J., Roesler, A. J., and
615 Petrescu, E. M.: The hydrogen and oxygen isotopic composition of precipitation,
616 evaporated mine water, and river water in Montana, USA, Journal of Hydrology,
617 328, 319–330, https://doi.org/10.1016/j.jhydrol.2005.12.005, 2006.
618 Gessner, M. O., Hinkelmann, R., Nützmann, G., Jekel, M., Singer, G., Lewandowski,
619 J., Nehls, T., and Barjenbruch, M.: Urban water interfaces, Journal of Hydrology,
620 514, 226–232, https://doi.org/10.1016/j.jhydrol.2014.04.021, 2014.
621 Gibson, J. J., Edwards, T. W. D., Birks, S. J., St Amour, N. A., Buhay, W. M.,
622 McEachern, P., Wolfe, B. B., and Peters, D. L.: Progress in isotope tracer
623 hydrology in Canada, Hydrol. Process., 19, 303–327,
624 https://doi.org/10.1002/hyp.5766, 2005.
625 Gibson, J. J. and Edwards, T. W. D.: Regional water balance trends and
626 evaporation-transpiration partitioning from a stable isotope survey of lakes in

627 northern Canada: REGIONAL WATER BALANCE USING STABLE
628 ISOTOPES, Global Biogeochem. Cycles, 16, 10-1-10–14,
629 https://doi.org/10.1029/2001GB001839, 2002.
630 Gibson, J. J., Prepas, E. E., and McEachern, P.: Quantitative comparison of lake
631 throughflow, residency, and catchment runoff using stable isotopes: modelling
632 and results from a regional survey of Boreal lakes, Journal of Hydrology, 2002.
633 Gillefalk, M., Tetzlaff, D., Hinkelmann, R., Kuhlemann, L.-M., Smith, A., Meier, F.,
634 Maneta, M. P., and Soulsby, C.: Quantifying the effects of urban green space on
635 water partitioning and ages using an isotope-based ecohydrological model,
636 Hydrol. Earth Syst. Sci., 25, 3635–3652,
637 https://doi.org/10.5194/hess-25-3635-2021, 2021.
638 Giri, S. and Qiu, Z.: Understanding the relationship of land uses and water quality in
639 Twenty First Century: A review, Journal of Environmental Management, 173,
640 41–48, https://doi.org/10.1016/j.jenvman.2016.02.029, 2016.
641 Grimm, N. B., Faeth, S. H., Golubiewski, N. E., Redman, C. L., Wu, J., Bai, X., and
642 Briggs, J. M.: Global Change and the Ecology of Cities, Science, 319, 756–760,
643 https://doi.org/10.1126/science.1150195, 2008.
644 Guan, M., Sillanpää, N., and Koivusalo, H.: Storm runoff response to rainfall pattern,
645 magnitude and urbanization in a developing urban catchment: Storm Runoff
646 Response to Rainfall Pattern, Magnitude and Urbanization, Hydrol. Process.,
647 n/a-n/a, https://doi.org/10.1002/hyp.10624, 2015.

Hamilton, S. K., Bunn, S. E., Thoms, M. C., and Marshall, J. C.: Persistence of aquatic refugia between flow pulses in a dryland river system(Cooper Creek, Australia), Limnol. Oceanogr., 50, 743–754, https://doi.org/10.4319/lo.2005.50.3.0743, 2005.

Han, S., Slater, L., Wilby, R. L., and Faulkner, D.: Contribution of urbanisation to non-stationary river flow in the UK, Journal of Hydrology, 613, 128417, https://doi.org/10.1016/j.jhydrol.2022.128417, 2022.

Jacobson, C. R.: Identification and quantification of the hydrological impacts of imperviousness in urban catchments: A review, Journal of Environmental Management, 92, 1438–1448, https://doi.org/10.1016/j.jenvman.2011.01.018, 2011.

Liu, J., Shen, Z., and Chen, L.: Assessing how spatial variations of land use pattern affect water quality across a typical urbanized basin in Beijing, China, Landscape and Urban Planning, 176, 51–63, https://doi.org/10.1016/j.landurbplan.2018.04.006, 2018.

Ma, H., Zhu, G., Zhang, Y., Sang, L., Wan, Q., Zhang, Z., Xu, Y., and Qiu, D.: Ion migration process and influencing factors in inland river basin of arid area in China: a case study of Shiyang River Basin, Environ Sci Pollut Res, 28, 56305–56318, https://doi.org/10.1007/s11356-021-14484-3, 2021.

Ma, J., Pan, F., Chen, L., Edmunds, W. M., Ding, Z., He, J., Zhou, K., and Huang, T.: Isotopic and geochemical evidence of recharge sources and water quality in the

669 Quaternary aquifer beneath Jinchang city, NW China, Applied Geochemistry, 25,
670 996–1007, https://doi.org/10.1016/j.apgeochem.2010.04.006, 2010.
671 Ma, X., Li, N., Yang, H., and Li, Y.: Exploring the relationship between urbanization
672 and water environment based on coupling analysis in Nanjing, East China,
673 Environ Sci Pollut Res, 29, 4654–4667,
674 https://doi.org/10.1007/s11356-021-15161-1, 2022.
675 Maavara, T., Chen, Q., Van Meter, K., Brown, L. E., Zhang, J., Ni, J., and Zarfl, C.:
676 River dam impacts on biogeochemical cycling, Nat Rev Earth Environ, 1,
677 103–116, https://doi.org/10.1038/s43017-019-0019-0, 2020.
678 Małoszewski, P., Rauert, W., Stichler, W., and Herrmann, A.: Application of flow
679 models in an alpine catchment area using tritium and deuterium data, Journal of
680 Hydrology, 66, 319–330, https://doi.org/10.1016/0022-1694(83)90193-2, 1983.
681 Martin, K. L., Hwang, T., Vose, J. M., Coulston, J. W., Wear, D. N., Miles, B., and
682 Band, L. E.: basin impacts of climate and land use changes depend on magnitude
683 and land use context, Ecohydrology, 10, e1870, https://doi.org/10.1002/eco.1870,
684 2017.
685 McDonough, L. K., Santos, I. R., Andersen, M. S., O'Carroll, D. M., Rutlidge, H.,
686 Meredith, K., Oudone, P., Bridgeman, J., Gooddy, D. C., Sorensen, J. P. R.,
687 Lapworth, D. J., MacDonald, A. M., Ward, J., and Baker, A.: Changes in global
688 groundwater organic carbon driven by climate change and urbanization, Nat
689 Commun, 11, 1279, https://doi.org/10.1038/s41467-020-14946-1, 2020.

McGlynn, B., McDonnell, J., Stewart, M., and Seibert, J.: On the relationships between catchment scale and streamwater mean residence time, Hydrol. Process., 17, 175–181, https://doi.org/10.1002/hyp.5085, 2003.

McGuire, K. J., McDonnell, J. J., Weiler, M., Kendall, C., McGlynn, B. L., Welker, J. M., and Seibert, J.: The role of topography on catchment-scale water residence time: CATCHMENT-SCALE WATER RESIDENCE TIME, Water Resour. Res., 41, https://doi.org/10.1029/2004WR003657, 2005.

Murgulet, D., Murgulet, V., Spalt, N., Douglas, A., and Hay, R. G.: Impact of hydrological alterations on river-groundwater exchange and water quality in a semi-arid area: Nueces River, Texas, Science of The Total Environment, 572, 595–607, https://doi.org/10.1016/j.scitotenv.2016.07.198, 2016.

Négrel, P., Petelet-Giraud, E., and Millot, R.: Tracing water cycle in regulated basin using stable $\delta^{18}O$–$\delta^{2}H$ isotopes: The Ebro river basin (Spain), Chemical Geology, 422, 71–81, https://doi.org/10.1016/j.chemgeo.2015.12.009, 2016.

Nolan, T. M., Reynolds, L. J., Sala-Comorera, L., Martin, N. A., Stephens, J. H., O'Hare, G. M. P., O'Sullivan, J. J., and Meijer, W. G.: Land use as a critical determinant of faecal and antimicrobial resistance gene pollution in riverine systems, Science of The Total Environment, 871, 162052, https://doi.org/10.1016/j.scitotenv.2023.162052, 2023.

Oudin, L., Salavati, B., Furusho-Percot, C., Ribstein, P., and Saadi, M.: Hydrological impacts of urbanization at the catchment scale, Journal of Hydrology, 559, 774–786, https://doi.org/10.1016/j.jhydrol.2018.02.064, 2018.

712 Peñas, F. J. and Barquín, J.: Assessment of large-scale patterns of hydrological
713 alteration caused by dams, Journal of Hydrology, 572, 706–718,
714 https://doi.org/10.1016/j.jhydrol.2019.03.056, 2019.
715 Peng, T.-R., Huang, C.-C., Wang, C.-H., Liu, T.-K., Lu, W.-C., and Chen, K.-Y.:
716 Using oxygen, hydrogen, and tritium isotopes to assess pond water's contribution
717 to groundwater and local precipitation in the pediment tableland areas of
718 northwestern Taiwan, Journal of Hydrology, 450–451, 105–116,
719 https://doi.org/10.1016/j.jhydrol.2012.05.021, 2012.
720 Pickett, S. T. A., Cadenasso, M. L., Grove, J. M., Boone, C. G., Groffman, P. M.,
721 Irwin, E., Kaushal, S. S., Marshall, V., McGrath, B. P., Nilon, C. H., Pouyat, R.
722 V., Szlavecz, K., Troy, A., and Warren, P.: Urban ecological systems: Scientific
723 foundations and a decade of progress, Journal of Environmental Management, 92,
724 331–362, https://doi.org/10.1016/j.jenvman.2010.08.022, 2011.
725 Qian, H., Dou, Y., Li, X.J., Yang, B.C., and Zhao, Z.H.: Changes of $\delta^{18}O$ and δD
726 along Dousitu River and its indication of river water evaporation. Hydrogeol.
727 Eng. Geol. 34 (1), 107–112,
728 https://doi.org/10.16030/j.cnki.issn.1000-3665.2007.01.024,2007.
729 Ren, L., Cui, E., and Sun, H.: Temporal and spatial variations in the relationship
730 between urbanization and water quality, Environ Sci Pollut Res, 21,
731 13646–13655, https://doi.org/10.1007/s11356-014-3242-8, 2014.
732 Rodgers, P., Soulsby, C., Waldron, S., and Tetzlaff, D.: Using stable isotope tracers to
733 assess hydrological flow paths, residence times and landscape influences in a

734 nested mesoscale catchment, Hydrol. Earth Syst. Sci., 9, 139–155,
735 https://doi.org/10.5194/hess-9-139-2005, 2005.
736 Salvadore, E., Bronders, J., and Batelaan, O.: Hydrological modelling of urbanized
737 catchments: A review and future directions, Journal of Hydrology, 529, 62–81,
738 https://doi.org/10.1016/j.jhydrol.2015.06.028, 2015.
739 Sang, L., Zhu, G., Xu, Y., Sun, Z., Zhang, Z., and Tong, H.: Effects of Agricultural
740 Large-And Medium-Sized Reservoirs on Hydrologic Processes in the Arid
741 Shiyang River Basin, Northwest China, Water Resources Research, 59,
742 e2022WR033519, https://doi.org/10.1029/2022WR033519, 2023.
743 Shastri, H., Paul, S., Ghosh, S., and Karmakar, S.: Impacts of urbanization on Indian
744 summer monsoon rainfall extremes, J. Geophys. Res. Atmos., 120, 496–516,
745 https://doi.org/10.1002/2014JD022061, 2015.
746 Skrzypek, G., Mydłowski, A., Dogramaci, S., Hedley, P., Gibson, J. J., and Grierson,
747 P. F.: Estimation of evaporative loss based on the stable isotope composition of
748 water using Hydrocalculator, Journal of Hydrology, 523, 781–789,
749 https://doi.org/10.1016/j.jhydrol.2015.02.010, 2015.
750 Sun, G., Caldwell, P. V., and McNulty, S. G.: Modelling the potential role of forest
751 thinning in maintaining water supplies under a changing climate across the
752 conterminous United States: Response of Water Yield to Forest Thinning and
753 Climate Change, Hydrol. Process., 29, 5016–5030,
754 https://doi.org/10.1002/hyp.10469, 2015.

Sun, G. and Lockaby, B. G.: Water Quantity and Quality at the Urban-Rural Interface, in: Urban-Rural Interfaces, edited by: Laband, D. N., Lockaby, B. G., and Zipperer, W. C., American Society of Agronomy, Soil Science Society of America, Crop Science Society of America, Inc., Madison, WI, USA, 29–48, https://doi.org/10.2136/2012.urban-rural.c3, 2012.

Sun, Z., Zhu, G., Zhang, Z., Xu, Y., Yong, L., Wan, Q., Ma, H., Sang, L., and Liu, Y.: Identifying surface water evaporation loss of inland river basin based on evaporation enrichment model, Hydrological Processes, 35, e14093, https://doi.org/10.1002/hyp.14093, 2021.

Talma, S, Woodborne, S. and Lorentz, S.: South African Contribution to the Rivers CRP, 2012.

UN-Habitat: World cities report 2020 : the value of sustainable urbanization, UN-Habitat, Nairobi, Kenya, 377 pp., 2020.

United Nations Department of Economic and Social Affairs: World Urbanization Prospects 2018: Highlights, United Nations, https://doi.org/10.18356/6255ead2-en, 2019.

Vitvar, T., Aggarwal, P. K., and Herczeg, A. L.: Global network is launched to monitor isotopes in rivers, Eos Trans. AGU, 88, 325–326, https://doi.org/10.1029/2007EO330001, 2007.

Vystavna, Y., Harjung, A., Monteiro, L. R., Matiatos, I., and Wassenaar, L. I.: Stable isotopes in global lakes integrate catchment and climatic controls on evaporation, Nat Commun, 12, 7224, https://doi.org/10.1038/s41467-021-27569-x, 2021.

777 Wang, B., Zhang, H., Liang, X., Li, X., and Wang, F.: Cumulative effects of cascade
778 dams on river water cycle: Evidence from hydrogen and oxygen isotopes,
779 Journal of Hydrology, 568, 604–610,
780 https://doi.org/10.1016/j.jhydrol.2018.11.016, 2019.
781 Wei, W., Shi, P., Zhou, J., Feng, H., Wang, X., and Wang, X.: Environmental
782 suitability evaluation for human settlements in an arid inland river basin: A case
783 study of the Shiyang River Basin, J. Geogr. Sci., 23, 331–343,
784 https://doi.org/10.1007/s11442-013-1013-y, 2013.
785 Westra, S., Fowler, H. J., Evans, J. P., Alexander, L. V., Berg, P., Johnson, F.,
786 Kendon, E. J., Lenderink, G., and Roberts, N. M.: Future changes to the intensity
787 and frequency of short-duration extreme rainfal, Rev. Geophys., 52, 522–555,
788 https://doi.org/10.1002/2014RG000464, 2014.
789 Wilson, C. and Weng, Q.: Assessing Surface Water Quality and Its Relation with
790 Urban Land Cover Changes in the Lake Calumet Area, Greater Chicago,
791 Environmental Management, 45, 1096–1111,
792 https://doi.org/10.1007/s00267-010-9482-6, 2010.
793 Wing, O. E. J., Bates, P. D., Smith, A. M., Sampson, C. C., Johnson, K. A., Fargione,
794 J., and Morefield, P.: Estimates of present and future flood risk in the
795 conterminous United States, Environ. Res. Lett., 13, 034023,
796 https://doi.org/10.1088/1748-9326/aaac65, 2018.

797 Yang, L., Ni, G., Tian, F., and Niyogi, D.: Urbanization Exacerbated Rainfall Over
798 European Suburbs Under a Warming Climate, Geophysical Research Letters, 48,
799 e2021GL095987, https://doi.org/10.1029/2021GL095987, 2021.
800 Yang, S. L., Zhang, J., and Xu, X. J.: Influence of the Three Gorges Dam on
801 downstream delivery of sediment and its environmental implications, Yangtze
802 River, Geophys. Res. Lett., 34, L10401, https://doi.org/10.1029/2007GL029472,
803 2007.
804 Yu, D., Shi, P., Liu, Y., and Xun, B.: Detecting land use-water quality relationships
805 from the viewpoint of ecological restoration in an urban area, Ecological
806 Engineering, 53, 205–216, https://doi.org/10.1016/j.ecoleng.2012.12.045, 2013.
807 Zhang, W., Wan, Q., Zhu, G., and Xu, Y.: Distribution of soil organic carbon and
808 carbon sequestration potential of different geomorphic units in Shiyang river
809 basin, China, Environ Geochem Health, 45, 4071–4086,
810 https://doi.org/10.1007/s10653-022-01472-w, 2023.
811 Zhu, G., Guo, H., Qin, D., Pan, H., Zhang, Y., Jia, W., and Ma, X.: Contribution of
812 recycled moisture to precipitation in the monsoon marginal zone: Estimate based
813 on stable isotope data, Journal of Hydrology, 569, 423–435,
814 https://doi.org/10.1016/j.jhydrol.2018.12.014, 2019.
815 Zhu, G., Sang, L., Zhang, Z., Sun, Z., Ma, H., Liu, Y., Zhao, K., Wang, L., and Guo,
816 H.: Impact of landscape dams on river water cycle in urban and peri-urban areas
817 in the Shiyang River Basin: Evidence obtained from hydrogen and oxygen
818 isotopes, Journal of Hydrology, 602, 126779,

819 https://doi.org/10.1016/j.jhydrol.2021.126779, 2021.